
Check for updates

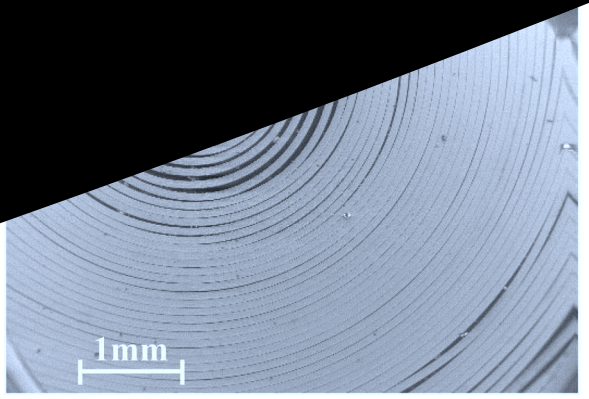

Fig. 2. SEM images of a) 1D and b) 2D realization of micro-structured tungsten concepts (top view).

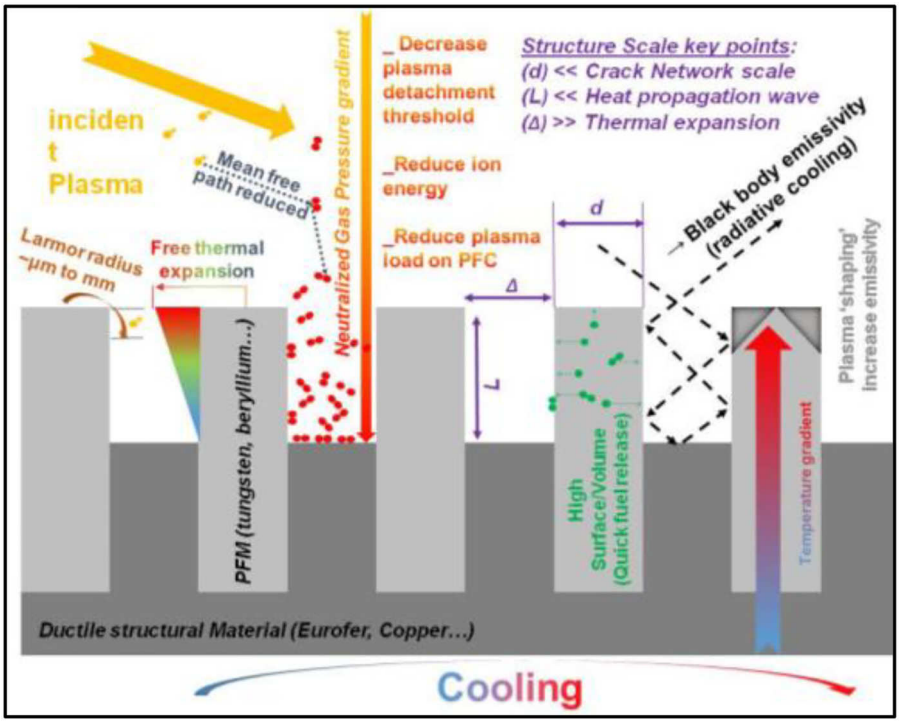

Fig. 1. Micro -structured tungsten concept principle (not to scale).

be dis-
monoblock, etc.),
tungsten is much less
pes in material as the PFM has
ratio in comparison to a traditional
average distance of trapped fuel to the surface
reduced and implies a much quicker and easier deso-
of fuel.

Sputtering itself needs to be also measured because it could annihilate any other benefits, as, because of the missing material, one could expect a shorter lifetime of a PFC using micro-structured tungsten. A question that authors are conscience of, and that, unfortunately, will not be answered in this paper, is whenever and how the eroded particles and dust, may fill gaps between fibres (co-deposits).

These two last points are critical when evaluating a PFC, as they are directly related to tritium inventory and PFC lifetime.

2.2. The prototypes

Two prototypes of micro-structured tungsten PFC were manufactured and tested. They were variations of the compact assembly of potassium doped tungsten fibres into a hexagonal lattice structure were investigated. The fibres used were 2.4 mm long in both cases having respectively 240 µm and 150 µm in diameter, to evaluate the influence of network lattice size on studied performances. Pure industrial grade copper was used to fill the gaps between the fibres (with 1.2 mm clearance from top) and to shape the samples to identical geometry to the reference bulk tungsten samples (PSI-2 compatible), resulting in an exposed surface of 10 × 10 mm^2 for plasma interaction and about 2000 and 5100 respectively, carefully aligned fibres. The top parts of the fibres have gaps about of 10 µm so they are not touching each others.

The reference sample was made from sintered and forged pure tungsten manufactured by Plansee according to ITER specifications with average (SEM measured) grain size between 1 and 10 µm, slightly elongated perpendicularly to the exposed surface. A more detailed characterisation can be found in [12]. The average grain size in the tungsten fibres was slightly smaller, being spread in an interval of 0.2–2 µm. The potassium doping might be responsible for some cracking observed during manufacturing and assembly, as it can be seen in Fig 2a). Finally, the top surface of all samples (micro-structured and bulk tungsten) was mechanically grinded, polished and finally electro-polished in 2 M NaOH solution in water to have identical mirror finished surfaces.

2.3. The experiments

These prototypes were exposed in the linear plasma facility PSI-2 to study plasma surface interaction but also for thermal shock

p
co
on
heig
cidenc
should
PFC and
and at th
lowering e
plasmas with

The distan g of the structural material has to e incident particles should not reach the st (more prone to erosion), b) to take advantage of the ed emissivity (sufficient absorption happen in 'gaps'), and c) to keep these advantages during the lifetime despite the inevitable erosion. However, this distance should be short enough for proper cooling to minimise the maximum temperature.

Spacing between structures behaves similar to a black body and increases the average emissivity of the PFC surface, improving the power handling at high temperatures. With a compact hexagonal lattice of tungsten fibres, one can expect an increase of emissivity from 0.24 for plain tungsten to 0.31, which represent about 29.5% of improvement (assuming black body radiation between fibres, gaps having multiple reflection like would in an Ulbricht sphere) which directly translate into a significant increase of the maximum heat flux that such a PFC could radiatively dissipate as shown in Fig. 3 (from 2.5 to 3.3 MW/m^2 at melting temperature). Last but not least, this emissivity should even increase over PFC lifetime due to the preferential sputtering of the edges of the fibres, which should lead to power handling

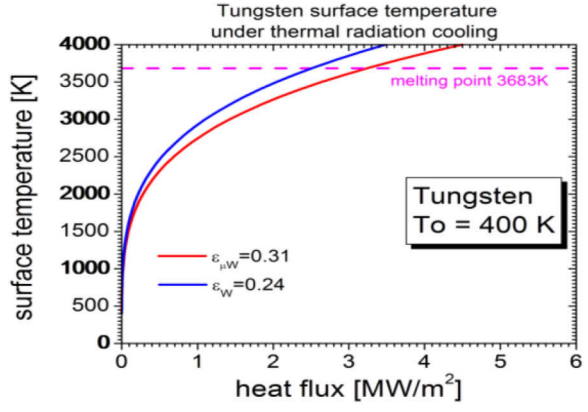

Fig. 3. Tungsten surface temperature versus radiative dissipation capability and emissivity.

Tab

s

gr

gasse

descri

used i

type K t

calibrate

15 μs time

used for the

spot.

For the ther

used (λ = 1064

spread homogene

quencies were between 0.5 Hz and 25 Hz and their duration of 1 ms (Table. 1). The base temperature of the samples (Fig. 3) was always below DBTT (230 °C maximum).

A partial mapping of each sample has been also made with SEM (resolution about 200 nm), while a complete mapping of the sample surface the identification of some fibre cracks was made with a metallographic optical microscope (resolution about 1 μm, 100 million pixel full mapping pictures) and compared before and after experiment. The pre- characterisation allowed to identify some cracks in fibres before any plasma exposure, which appear owing to the manufacturing process mostly during the last step of preparation by electro-polishing. Generally, this allowed tracking global and local morphology changes before and after experiments, like dust formation, erosion, and melting, but also changes of tungsten grains.

3. Experimental results

3.1. Steady state power handling

The first result of this experiment was to compare the temperatures of the plain bulk tungsten sample and the 240 μm micro-structured sample. Both samples showed during the experiment the same behaviour, same temperatures but the micro-structured sample appeared significantly brighter on the IR image which was expected from higher emissivity. However, the temperature range during experiments was clearly too low (25 °C to 350 °C) to see any benefits from higher emissivity by higher radiative cooling (i.e., no cooler temperature measured by thermocouple). It was also confirmed by Ansys simulations that in such configuration (steady state plasma), but even also in transient ones, both samples have almost the same temperatures (extremum and distribution): for example, 358 °C max and 198 °C min for bulk sample to compare with 335 °C max and 206 °C min for micro-structured sample (with copper base), both as steady state temperatures calculated for the transient δ case (Section 3.4).

assessed for micro-structured

more surface for plasma interaction

gle) which logically could result in higher

capture, but should also ease their release by thermal

. The key factor here is the temperature, because when the

mperature increase the total fuel inventory stored is reduced in the PFC due to a quick diffusion of hydrogen isotopes to the surface and desorption. A first evaluation of the influence of micro-structuring on fuel retention was carried with low steady state temperature of about 180 °C.

Both reference and micro-structured samples were exposed simultaneously to deuterium plasma of 51 eV during about 150 min for a total fluence of 5.1×10^{25} D^+ m^{-2}. All samples were exposed to the normal incident plasma flux. The total retention measured by TDS was by 59.6% higher for the micro-structured sample in comparison with the reference samples, though the total surface area is a factor 7 higher. This is due to the fact that D can be desorbed from a wider area than the bulk W surface. A moderate (+14.9%) increase of near surface retention in the micro-structured sample measured by μNRA can be explained by a slightly smaller grain structure prone to some higher deuterium capture.

3.4. ELMs and thermal fatigue

The previous experiments demonstrated that micro-structured tungsten behaves very similarly to bulk tungsten in terms of sputtering and in same range concerning the fuel retention, but its main advantage over them concerning the thermal fatigue has to be verified. To evaluate it, micro-structured and bulk tungsten were exposed to different number of laser pulses (Table 1 for parameters), to simulate ELMs events.

These ELMs like simulation has been performed in the same protocol as described in [12,10,2]. In this particular case, the laser pulses were sequential to the plasma exposure, but without venting the PSI-2 chamber. The evolution of the surface temperature of the micro-structured tungsten sample due to laser pulse irradiation measured by fast pyrometer is shown on Fig. 6. The post experimental analysis shows that even 10^5 pulses of 0.50 GW/m^2 were not enough to reach the damage threshold of micro-structured tungsten (Fig. 5) as no single crack newly appeared. It is important to remind that, as it was previously determined and evaluated [2], but also again confirmed in this experiment with the reference samples, the damage threshold, at such ELMs representative power densities, of the bulk ITER grade tungsten, is below 10 pulses. This micro-structuring represents an improvement factor of at least 10^4 for given low temperatures. The exact positions of the laser spots on micro-structured sample can be identified by tracking

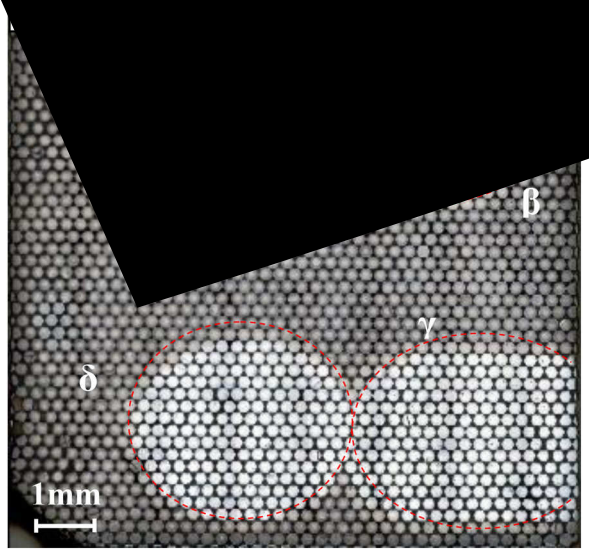

Fig. 5. Micrograph of samples after test irradiation at 10, 100, 1000 and 10,000 pulses.

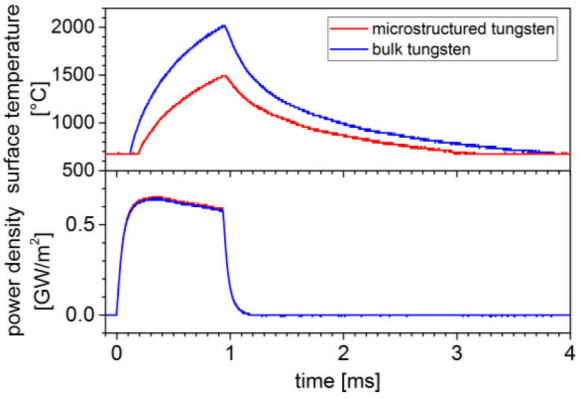

Fig. 6. Time traces of the surface temperature of micro-structured and reference tungsten sample and the laser power ($\sim 10^4$ pulse).

the molten particles in the gaps as well as by oxidation pattern, which appeared after a few days and spreading differently over exposed and un-exposed areas, likes shown Fig 5b).

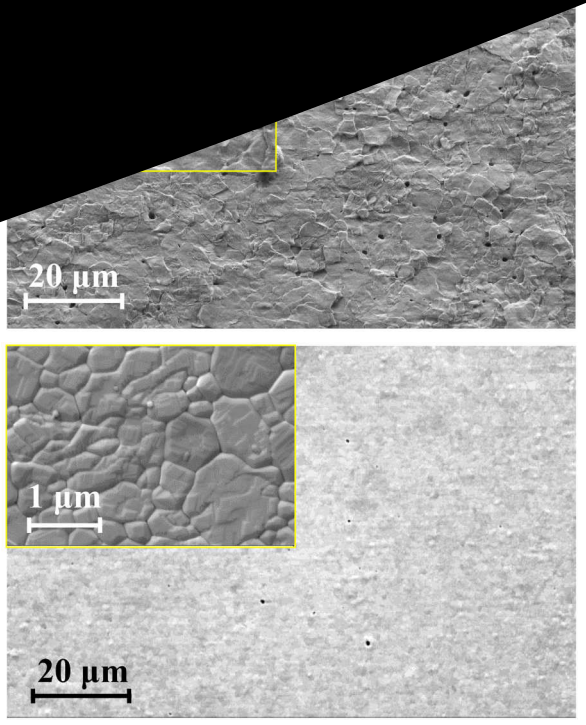

Fig. 8. SEM of bulk (top) and μ-structured (bottom) sample.

This can be affirmed as SEM of bulk sample reveal roughness increase and overlapping of thermal cycled tungsten grains but also an increase of their size (some grains reached 20 µm, with a starting size between 1 and 5 µm) while on micro-structured side, grains remains unchanged in their size (between 1 and 0.2 µm) and disposition (slightly larger in fibre centre than on edges) (Fig. 7).

4. Conclusions

The evaluation demonstrates that the micro-structured tungsten is a great improvement compared to bulk tungsten in the field of thermal fatigue caused by ELMs. Additionally, this improvement of more than a factor 10^4, comes without any particular drawback over ITER grade bulk tungsten, which in other words, means that it would perform, at least as well, in the others important concerns (fuel retention, sputtering, power handling…). The increase measured in deuterium retention can appear significant but has to be considered in perspective with the magnitude of order of the increase found in thermal cycling tests (+51% vs $+10^6$%). Additionally, this particular aspect can be significantly improved.

References

[1] Th. Loewenhoff, H. Maier, T.W. Morgan, G. Pintsuk, R.A. Pitts, B. R… ed transient plasma/heat loads on tungsten performance be… recrystallization temperature, Nucl. Fusion 55 (2015) 123004, … https://doi.org/10.1088/0029-5515/55/12/123004.

[2] M Wirtz, A. Kreter, J. Linke, Th. Loewenhoff, G. Pintsuk, G. Sergienko, I. Steudel, B. Unterberg, E. Wessel, High pulse number thermal shock tests on tungsten with steady state particle background, Phys. Scr. (2017) 014066, , https://doi.org/10.1088/1402-4896/aa909e T170.

[3] V.P. Budaev, Results of high heat flux tests of tungsten divertor targets under plasma heat loads expected in ITER and tokamaks, Phys. Atomic Nuclei 79 (7) (2016) 1137–1162, https://doi.org/10.1134/S106377881607005X.

… Burdakov, …ps, G. Pintsuk, M. Reinhart, …M. Zlobinski, Investigation of the … laser irradiation on ITER-grade tungsten, … 10.1088/0031-8949/2014/T159/014005

… physical processes and reduced models for plasma detachment, …ys. Control. Fusion 60 (2018) 044022, , https://doi.org/10.1088/1361-…//aaacf6.

[12] M. Wirtz, I. Uytdenhouwen, V. Barabash, F. Escourbiac, T. Hirai, J. Linke, Th. Loewenhoff, S. Panayotis, G. Pintsuk, Material properties and their influence on the behaviour of tungsten as plasma facing material, Nucl. Fusion 57 (2017) 066018, , https://doi.org/10.1088/1741-4326/aa6938.

[13] A. Kreter, C. Brandt, A. Huber, S. Kraus, S. Moeller, M. Reinhart, B. Schweer, G. Sergienko, B. Unterberg Linear plasma device PSI-2 for plasma-material interaction studies, Fusion Sci. Technol. 68(1) (2015) 8–14, doi.org/10.13182/FST14-906.

[14] A. Gorshkov, K. Vukolov, I. Bel.bas, M. Maslov, V. Sannikov, Laser damage thresholds of single crystal tungsten mirror, 30th EPS Conference on Contr. Fusion and Plasma Phys. 27A St. Petersburg, 2003, pp. 7–11 JulyECAP-2.82.

[15] A. Litnovsky, T. Wegener, F. Klein, C. Linsmeier, M. Rasinski, A. Kreter, B. Unterberg, J.W. Coenen, H. Du, J. Mayer, C. Garcia-Rosales, A. Calvo, N. Ordas, Smart tungsten alloys as a material for the first wall of a future fusion power plant, Nucl. Fusion 57 (6) (2017) 1363–1367, https://doi.org/10.1016/j.nme.2016.11.015.